Applied Thermal Engineering 198 (2021) 117466

Contents lists available at ScienceDirect

Applied Thermal Engineering

journal homepage: www.elsevier.com/locate/apthermeng

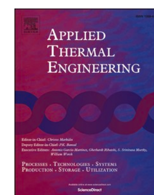

Design of a novel LED bulb with entire surface thermally activated for passive cooling

Shangsheng Feng [a,b], Zhuoran Liu [c], Baoming Cheng [d], Shanyouming Sun [e], Tian Jian Lu [f,g,*], Feng Xu [a,b,*]

[a] Key Laboratory of Biomedical Information Engineering of Ministry of Education, School of Life Science and Technology, Xi'an Jiaotong University, Xi'an 710049, PR China
[b] Bioinspired Engineering and Biomechanics Center (BEBC), Xi'an Jiaotong University, Xi'an 710049, PR China
[c] School of Aerospace Engineering, Tsinghua University, Beijing 100084, PR China
[d] Shanghai Institute of Quality Inspection and Technical Research, Shanghai 201100, PR China
[e] State Key Laboratory for Strength and Vibration of Mechanical Structures, Xi'an Jiaotong University, Xi'an 710049, PR China
[f] State Key Laboratory of Mechanics and Control of Mechanical Structures, Nanjing University of Aeronautics and Astronautics, Nanjing 210016, PR China
[g] MIIT Key Laboratory of Multi-functional Lightweight Materials and Structures, Nanjing University of Aeronautics and Astronautics, Nanjing 210016, PR China

A R T I C L E I N F O

Keywords:
LED lighting
Energy saving
Thermal design
Chimney effects
Electronics cooling

A B S T R A C T

LED lightings have made significant contributions to global energy saving, where one major challenge is the overheating of LED chips since the light output and lifespan of LED chips decrease exponentially with increasing operating temperature. Restricted by cooling capacity, the power input and light output of a LED bulb is limited. At present the luminous flux of commercial LED bulbs (A19 size) is usually limited to 800 lm with the related power consumption within 9 W. Therefore, there is an urgent market need for high-lumen bulbs while maintaining the size and shape as conventional incandescent bulbs. We report herein a novel design which could make full use of the entire outer surface of LED bulb as heat dissipating surface under passive cooling conditions. The novel design contains a chimney inside the bulb and an external heat sink, enabling two parallel heat dissipating paths, *i.e.*, *chips - heat sink - environment* and *chips – chimney – lampshade - environment*. In conventional design with an external heat sink for cooling, the lampshade functions only to transmit light rather than dissipate heat. However, in the novel design the chimney inside the bulb could thermally activate the lampshade to dissipate heat as well. Upon properly distributing thermal loads to the two heat dissipating paths, cooling capacity of the novel bulb was optimized. With this design strategy, the passive cooling capacity was significantly improved to be 1.57 times higher than the conventional design and the commercially available bulbs of the same size and shape. Most importantly, the design strategy may be extended to other passive cooling scenarios such as indoor small cells for 5G communication.

1. Introduction

The rapid growth of world energy consumption and its impact on environment have attracted much attention to energy conservation [1]. Grid based electric lighting consumes 19% of total global electricity production [2], and constitutes up to 20–40% of the total energy consumption in buildings [3]. The energy demand will continue to increase with the continuous growth of population, increasing demand for buildings comfort and the rise of time spent inside the building [1]. Therefore, it is of great importance to upgrade lighting devices to address energy and environmental challenges by using energy-saving light sources and proper lighting control system [4]. Light-emitting diodes (LEDs) have shown great potential as an energy-saving lighting source, due to its long lifespan, dynamic lighting effect and great design flexibility [5]. Compared to traditional fluorescent lamps, LED lamps use 75% less energy but have 9–10 times longer lives [4], which achieve 56% to 62% energy savings in a typical six-story office building [6]. LEDs are therefore considered to be the next generation of lighting

* Corresponding authors at: State Key Laboratory of Mechanics and Control of Mechanical Structures, Nanjing University of Aeronautics and Astronautics, Nanjing 210016, PR China (Tian Jian Lu). Key Laboratory of Biomedical Information Engineering of Ministry of Education, School of Life Science and Technology, Xi'an Jiaotong University, Xi'an 710049, PR China (Feng Xu).

E-mail addresses: tjlu@nuaa.edu.cn (T.J. Lu), fengxu@mail.xjtu.edu.cn (F. Xu).

https://doi.org/10.1016/j.applthermaleng.2021.117466
Received 5 February 2021; Received in revised form 20 July 2021; Accepted 14 August 2021
Available online 20 August 2021
1359-4311/© 2021 Published by Elsevier Ltd.

technology. For instance, China's LED industry started in the 1970s and dominated the entire lighting industry after more than ten years of rapid development [7]. The market share of LED lighting is gradually growing nowadays in China in terms of various application scenarios such as reading lights, window lights, outdoor lightings, spotlights, household lightings, automotive headlights *etc* [7]. However, overheating is the major threat to the lifespan and performance of LED chips which convert nearly 80% of the input electrical power into heat and the rest into light [8]. The operating temperature of LED chips determines its reliability, durability and efficiency, because the light output and lifespan exponentially decrease as the chip temperature increases [5]. High temperature would also cause significant thermal stress and failure at the interface of the chips [9]. Therefore, it is of great importance to develop efficient cooling technologies for LED lighting.

To keep the operating temperature lower of a certain value between 100 and 110 °C (since semiconducting materials can't resist high temperatures) [10], various cooling strategies have been developed by using either active cooling (*e.g.*, liquid cooling [11,12], jet impingement [13], forced air convection [14], microspray cooling [15], liquid metal [16], ionic wind cooling [14], piezoelectric fan [17]) or passive cooling technologies (*e.g.*, heat pipes [18,19], heat sinks [20–23], metal foam [24–26], thermal interface materials [14,27]). Although the active cooling approaches usually have higher cooling capacity than the passive cooling, they need a pump or fan to drive the motion of cooling fluid. By contrast, the passive cooling technologies are more reliable, cost-effective and lightweight [28], thus are more preferable for LED bulbs subjected to strict space and weight constrains. Conventional LED bulbs usually use a heat sink (termed as metal block hereafter) for heat dissipation, as shown in Fig. 1**(a)**. To enhance the cooling capacity, some designs installed extruded fins on the external surface of the metal block [5]. Other efforts included utilizing the venting or chimney effects to enhance the heat transfer of bulbs. For example, Jang *et al.* [29] installed a vertically aligned structure of PCB inside the bulb with perforated vents on the lampshade of the bulb. Petroski [10] proposed a hollow cylindrical shaped LED bulb which resembled to a chimney. Feng *et al.* [30] installed a chimney-like frame inside the LED bulb to enhance the heat transfer inside the bulb as shown in Fig. 1**(b)**, which thermally activated the external surface of the lampshade for heat dissipation to environment.

Despite numerous efforts have been made for cooling the LEDs, it is still challenging to design high-lumen LED bulbs such as 75 W and 100 W equivalent to incandescent bulbs while maintaining the size and shape of the bulb as the conventional products [10]. At present the luminous flux of commercial LED bulbs whose size meets the A19 standard is usually limited to 800 lm with the related power consumption within 9 W [31]. The difficulty of thermal design for LED bulbs is due to the size and shape of the bulb are subjected to strict constrains [10]. Although the active cooling (such as fan or liquid cooling) methods are efficient, they are not desirable for light bulbs from a consumer point view. The existing passively cooled high-lumen bulbs usually require larger sizes, failing to meet the size and shape constraints. Therefore, it is meaningful to increase the passive cooling capacity while maintaining the size and shape of the bulbs.

In this paper, we proposed a novel design of LED bulb with a passive cooling capacity of 11.7 W (corresponding to a power input of 14.6 W), which is 1.57 times higher than the conventional bulb of the same size and shape. The novel design contains a chimney inside the bulb and an external heat sink (*i.e.*, heat dissipating metal block) for cooling, thus

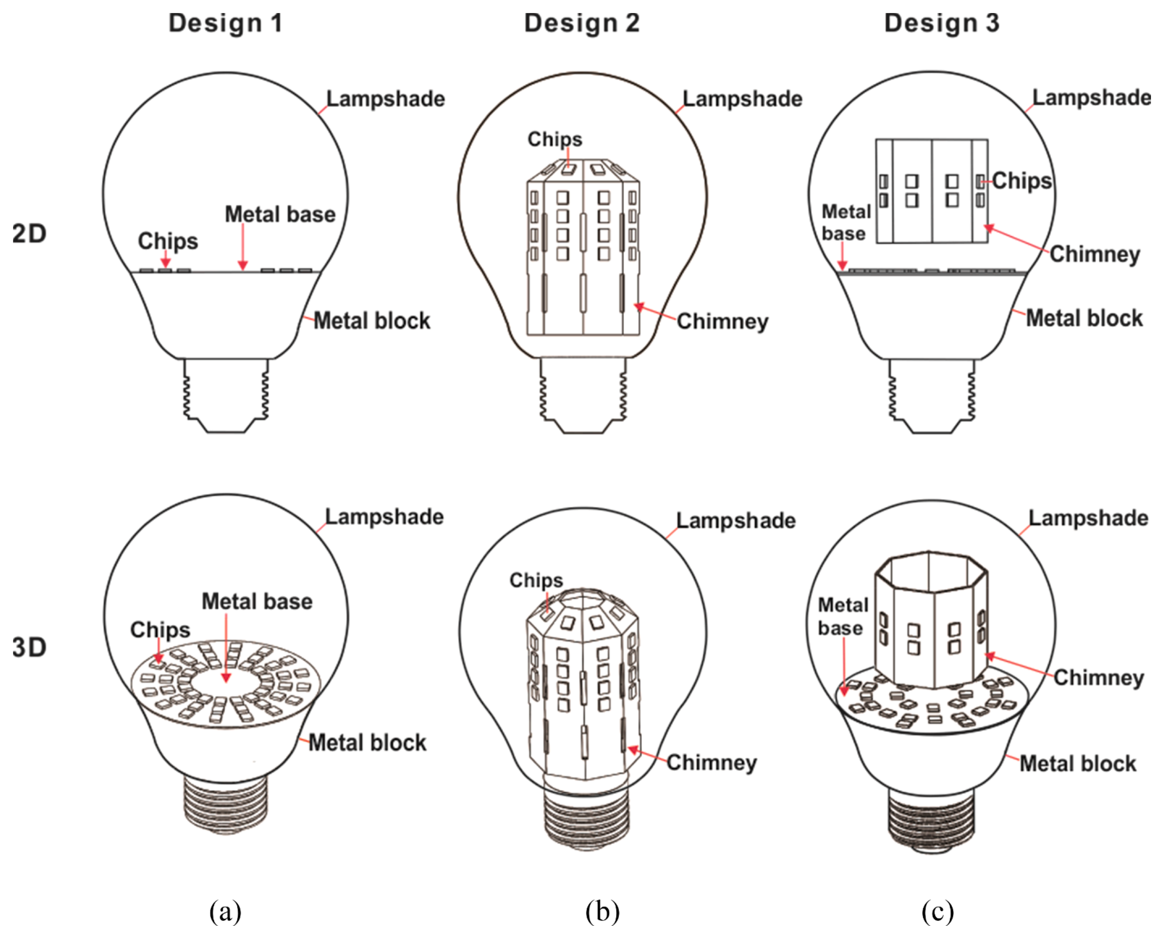

Fig. 1. Schematics of the three conceptual designs of LED bulbs investigated in the study: (a) conventional LED bulb with only a metal block for passive cooling; (b) chimney-based passive cooling bulb; (c) present novel bulb combining a metal block and a chimney for enhanced passive cooling.

can make full use of the entire outer surface of the bulb exposed to the surroundings for heat dissipation. For comparison, three conceptual designs of bulb configurations were considered with the same size and shape: 1) conventional bulb with only a metal block for heat dissipation; 2) bulb with only a chimney and 3) the novel design with both a chimney and a metal block. The remaining sections of the paper is organized as follows. In Section 2 the three conceptual designs are introduced. The Section 3 presents the numerical model used to evaluate the cooling capacity of the bulbs. The cooling capacity, heat transfer mechanisms and optimization of the considered LED bulbs along with comparison with Philips bulbs are discussed in Section 4, followed by conclusions in Section 5.

2. Three conceptual designs of LED bulbs

For comparison, three conceptual designs of LED bulbs were investigated, including the conventional bulb with only a heat dissipating metal block, the bulb with only a chimney [30], and the novel design containing a metal block and a chimney (Fig. 1). For fair comparison, the three configurations had exactly the same size and shape as the bulb investigated by the authors in Ref. [30]. In the conventional design (design 1), as shown in Fig. 1**(a)**, the waste heat of the chips was first conducted to the metal base then to the metal block and finally dissipated to the environment. For the bulb with only a chimney (design 2), as shown in Fig. 1**(b)**, the waste heat of the chips was first transferred to the chimney then from the chimney to the inner surface of the lampshade and finally dissipated to the environment from outer surface of the lampshade. For the novel bulb design 3, as shown in Fig. 1**(c)**, part of waste heat from the chips was released to the environment by the metal block and the remaining by the lampshade. More details on the configurations of the three designs were summarized as below:

(1) The conventional bulb (*i.e.*, design 1) contained a lampshade, a metal base, a metal block and 48 LED chips, where all the chips were placed on the metal base whose periphery was thermally contact with the metal block.
(2) The bulb with only a chimney (*i.e.*, design 2) contained a lampshade, a chimney and 48 LED chips placed on the chimney. The chimney was a metallic, hollow, eight-sector revolving body with a contraction neck at the top. The top neck was initially designed for placing several chips to ensure uniform light emission from the bulb [30].
(3) The present novel bulb (*i.e.*, design 3) included a lampshade, a metal base, a metal block, a chimney and 48 LED chips [32], where some chips were placed on the metal base and the others on the chimney. The chimney was straight without contraction neck at the top. To allow uniform light emission, several chips were placed at the center of the metal base.

It is worthy to note that the chimney in design 2/3 was connected to the base of bulb with a wire-frame made of thin metal. It was found that the wire-frame did not influence thermal and fluid flow in the bulb. Therefore, the wire-frame was not simulated in the model.

3. Numerical methods

In this section, the numerical methods for evaluating the passive cooling capacity of the above LED bulbs are detailed.

3.1. Computational domain, governing equations and boundary conditions

The entire heat dissipation process of LED bulbs includes heat transfer in the bulb and coupled heat transfer between the bulb and the atmosphere. Correspondingly, the computation domain should cover each necessary components of the bulb, gas domain inside the bulb and outside air enveloping the bulb (Fig. 2). The outside sphere of air domain should be big enough to avoid any size effects, whose radius was varied from two to five times the height of the bulb with negligible effects found. Due to the rotational periodic structure of the bulbs, the computational domains have only covered the minimum unit cell of a bulb (*i.e.*, 1/16, 1/8, 1/4 of the whole bulb for the design 1/2/3, respectively) to save the computational cost. The sub-domains alone with their materials make for the three designs are listed in Table 1.

The problem involves heat conduction, natural convection and radiation heat transfer. Standard heat conduction equation was used for heat transfer in solid components of the bulb such as LED chips, metal base/block, lampshade, *etc*. Navier-Stokes equations with buoyancy force term were used for natural convection both inside and outside the bulb. The discrete ordinates model (DO model) which supports periodic and symmetry boundary conditions was chosen to determine radiative heat flux in the energy equation. More details on the numerical model can be referred to our previous work [30]. Other assumptions made to complete the numerical model are summarized as below:

(1) The flow was three-dimensional, laminar and steady;
(2) Densities of the gases were computed using ideal gas law, while other relevant thermal physical properties of the gases were temperature dependent;
(3) Thermal physical properties of the solids were constant;
(4) The gases were optically thin and transparent to thermal radiation;
(5) The lampshade (made of glass) and LED chips were opaque media and optically thick, therefore thermal radiation could not transmit through them;
(6) All solid surfaces were gray and diffuse.

Based on the above assumptions, governing equations are listed as below [30].

Continuity equation:

$$\nabla\cdot(\rho \boldsymbol{v}) = 0 \tag{1}$$

Momentum equation:

$$\rho\frac{D\boldsymbol{v}}{Dt} = -\nabla p + \eta\nabla^2\boldsymbol{v} + \boldsymbol{F}\,(forz - direction\,\boldsymbol{F}_z = -\rho g) \tag{2}$$

Energy equation:

$$\rho c_p\frac{DT}{Dt} = \nabla\cdot(\lambda\nabla T) + S_h \tag{3}$$

Radiative transfer equation (DO model):

$$\nabla\cdot(I(\overrightarrow{r},\overrightarrow{s})\overrightarrow{s}) + (a+\sigma_s)I(\overrightarrow{r},\overrightarrow{s}) = an^2\frac{\sigma T^4}{\pi} + \frac{\sigma_s}{4\pi}\int_0^{4\pi} I(\overrightarrow{r},\overrightarrow{s}')\Phi(\overrightarrow{s}\cdot\overrightarrow{s}')d\Omega' \tag{4}$$

Solid region energy equation:

$$\nabla\cdot(\lambda\nabla T) + S_h = 0 \tag{5}$$

where **v** is the velocity vector, p is the fluid pressure, **F** is the buoyancy force, g is the gravity acceleration, and T is the temperature; ρ, c_p, and η are the density, specific heat and viscosity of gas, respectively. λ is the thermal conductivity. I is the radiation intensity depending on the position vector ($\overrightarrow{r}$) and direction vector ($\overrightarrow{s}$). σ is the Stefan-Boltzmann constant. a, σ_s, and n are the absorption coefficient, scattering coefficient and refractive index respectively of each medium. For gas medium, they were set to be 0, 0, 1 respectively, due to the transparent assumption. For the solid medium, these coefficients will not influence the computational results since radiation could not transmit through the solid boundaries. While S_h in Eq. (3) represents the radiation source term, the coupling strategy between the energy equation and the radiation equation can be referred to Ref. [33]. Volumetric heat source (S_h)

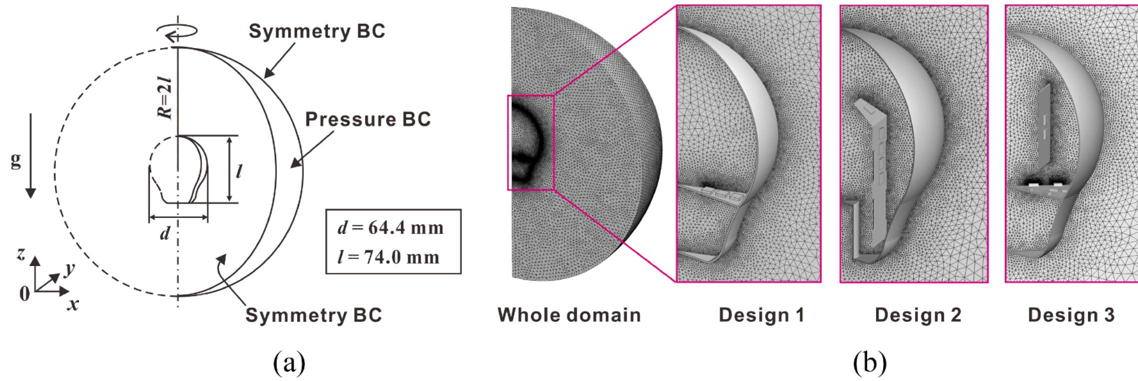

Fig. 2. Numerical model: (a) computational domain and (b) computational mesh used in the numerical simulation.

Table 1
Sub-domains for the three designs of bulbs along with the materials make.

Sub-domains	LED chips	Metal base	Metal block	Chimney	Lampshade	Gas inside bulb	Outer sphere
design 1	yes	aluminium	aluminium	no	glass	air /optimum mixture gas	air
design 2	yes	no	no	aluminium	glass	air/optimum mixture gas	air
design 3	yes	aluminium	aluminium	aluminium	glass	air/optimum mixture gas	air

in Eq. (5) was used for LED chips to simulate the waste heat.

The thermal conductivities of LED chips, glass and aluminum were set to be 147 W/(m·K), 0.7 W/(m·K) and 202.4 W/(m·K), respectively. Unless specified, the bulb was filled with air. The thermal conductivity, viscosity and specific heat of air were correlated as functions of the temperature as [34]:

$$\lambda = (0.0067T + 0.6172) \times 10^{-2} \tag{6}$$

$$\eta = (0.0429T + 5.8441) \times 10^{-6} \tag{7}$$

$$c_p = 0.0004T^2 - 0.2013T + 1031.1 \tag{8}$$

In some cases, the bulbs were filled with a mixture of 73% helium and 27% xenon (termed as the “optimum gas mixture” thereafter) which could maximize the natural convection heat transfer inside the bulb [30]. The thermal conductivity, viscosity and specific heat of the optimum gas mixture were calculated using the formula given in Ref. [30].

Pressure inlet boundary condition was prescribed at surface of the outer sphere with ambient pressure and temperature to simulate the free ambient condition. Volumetric heat source was imposed for each LED chip. Since all LED chips were connected in series, the volumetric heat source of each chip was assumed identical. Non-slip boundary condition was applied at all the solid–fluid interfaces, with unity emissivity set at each interface.

3.2. Numerical methods

A multi-block unstructured mesh incorporating fully tetrahedral elements was generated in Gambit 2.4.6 for all the sub-domains (Fig. 2). Grid density should be fine enough to resolve the velocity and temperature gradients in the domain. Usually, large velocity and temperature gradients exist nearby a solid surface due to flow and thermal boundary layers. Therefore, the mesh nearby a solid surface should be refined to resolve the boundary layers whilst the mesh density in the core can be smaller to save the computational cost. To this end, a non-uniform mesh was generated using the “size function” embedded in Gambit as shown in Fig. 2. To check the grid independency, the number of elements was tested from 1 million to 4 million, and the results showed no difference.

A commercial CFD code (ANSYS Fluent 14.5) was used to solve the current problem as formulated. Since pressure variation was insignificant compared to temperature variation in the problem, incompressible-ideal-gas law was chosen for the density of gases. The SIMPLE algorithm was applied to couple the pressure and velocity for numerical analysis. A second-order upwind scheme was applied to discretize the convective terms of governing equations. The values of angular discretization and pixilation were set to be 4 × 4 and 3 × 3 respectively in Fluent [30]. The iterative convergence criterion was chosen as 10^{-3} for momentum equation and 10^{-6} for energy equation, which had been verified to be small enough to ensure the prediction results independent of the selected values.

The numerical results of design 2 had been validated against experimental results in our previous study [30]. Since exactly the same numerical setup and meshing strategy were applied for design 2 and other configurations, the simulation results in the present study would be credible.

4. Results and discussion

The numerical methods used to evaluate the cooling capacity of LED bulbs have been described in Section 3. In this section, thermo-fluid flow distributions, heat transfer mechanisms and cooling capacity of the three bulb designs is presented first in Section 4.1. Then the novel configuration of design 3 is optimized by altering the chip distribution and structure of chimney, which will be presented in Section 4.2. Finally, the optimal bulb of design 3B is compared with existing bulbs in Section 4.3.

4.1. Thermo-fluid flow distributions, heat transfer mechanisms and cooling capacity of the three designs of bulbs

4.1.1. Thermo-fluid flow distribution characteristics

Fig. 3(a-c) present flow streamlines and temperature distributions of the gas filled in the three LED bulbs, respectively. Given the same thermal load of 7 W, the gas temperature in design 2 was significantly higher than the other two designs, which can be explained by the fact that in design 2 there was no metal block to conduct out the waste heat. By contrast, in the design 1/3 with a heat dissipating metal block, part of waste heat was conducted out of the bulbs by the metal blocks, so less heat was transferred into the gas inside the bulb. Therefore, it is preferable to maintain the heat dissipating metal block to reduce the temperature level inside the LED bulb. Moreover, flow circulations can be clearly observed in all of the three bulbs due to natural convection of gas

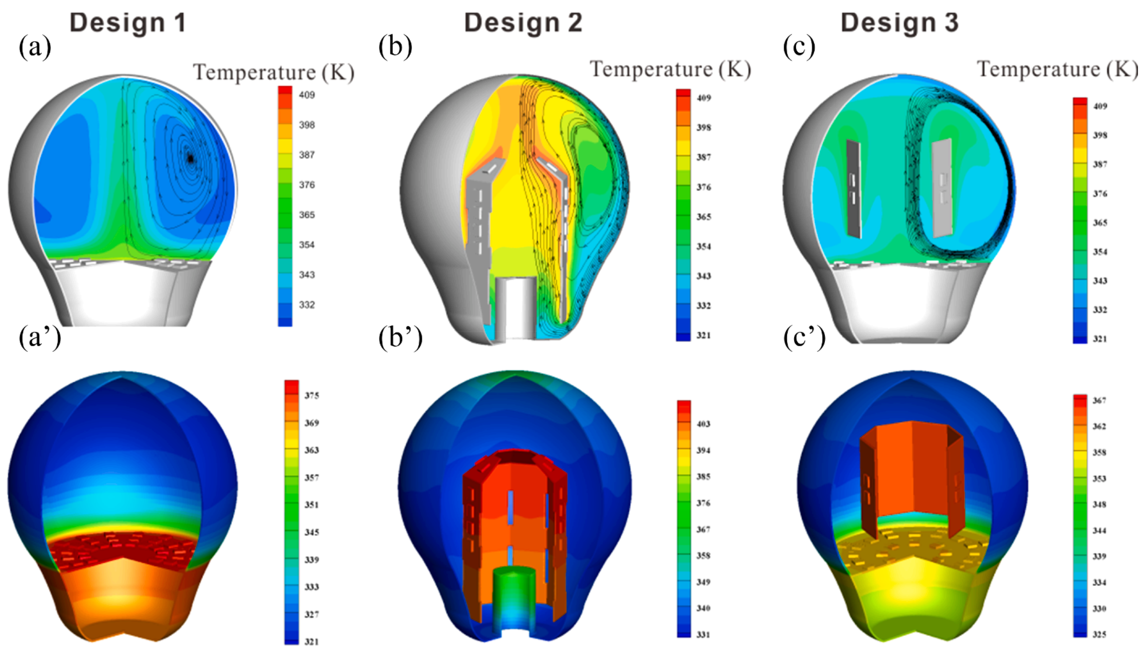

Fig. 3. Numerical results for temperature and streamline distributions of gas inside bulbs of design 1–3 (a-c) and for temperature distributions of solids (a'-c') of the three bulbs. All bulbs were filled with air at a thermal load of 7 W.

within the bulbs. However, natural convection flow in design 2 and 3 was intensified by the chimney structure in comparison to design 1, which can be inferred from the different densities of flow streamlines of the three bulbs.

Fig. 3(a'-c') show temperature distributions of solid components of the three designs of bulbs respectively. For the bulb of design 1, the highest temperature located at the metal base where the chips were placed on, followed by the metal block and the lampshade. For the design 2 with a chimney, the hottest component was the chimney; and temperature level on the lampshade was significantly higher than that of design 1, indicating more heat dissipation from the lampshade. For the design 3, since the chips were distributed on the chimney and the metal base, the two components were both heated up thus enabling two heat dissipation paths: *chips – chimney – lampshade – environment* and *chips - metal base - metal block - environment*.

4.1.2. Heat transfer mechanisms

A deep understanding of heat transfer process can help to optimize the thermal design. To understand the heat transfer mechanisms within the bulbs, Fig. 4 presents the heat dissipation paths of the three bulbs

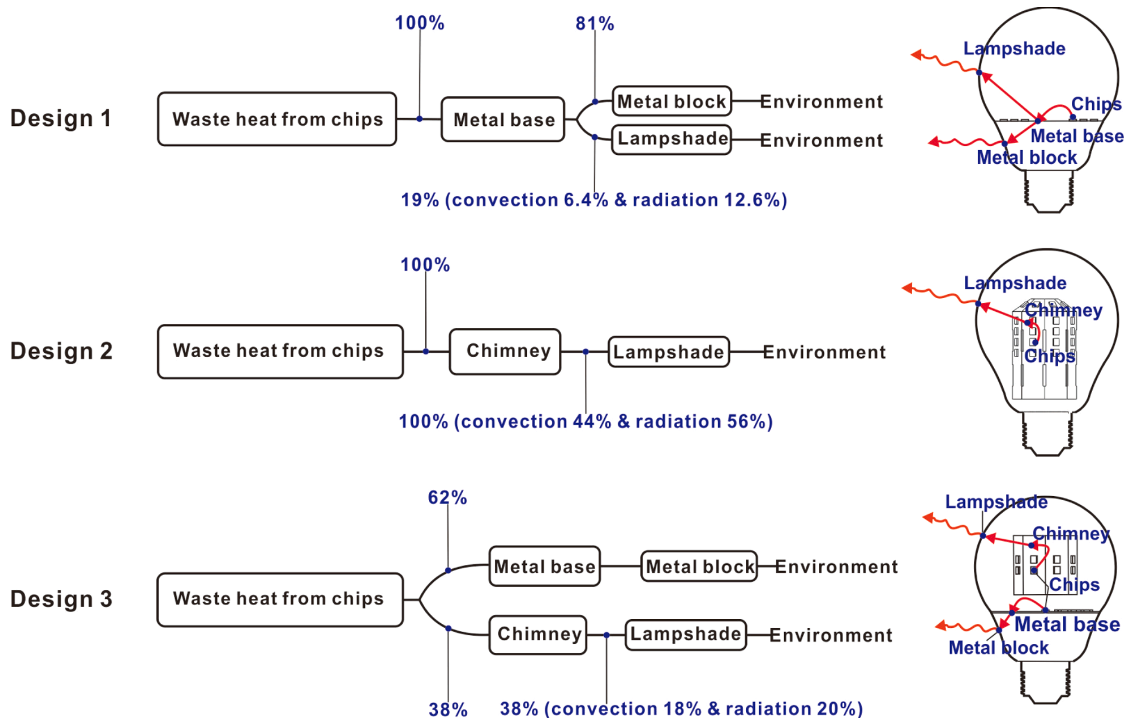

Fig. 4. Contribution of each heat transfer path to the total heat dissipation for the three designs of bulb.

along with the contribution of each heat transfer process.

As shown in Fig. 4 for design 1, most of the waste heat (81%) from the LED chips was conducted out by the metal base to the metal block and eventually rejected from the metal block to the environment. The remaining waste heat (19%) was transferred from the metal base to the inner surface of lampshade *via* natural convection (6.4%) and radiation (12.6%) heat transfer inside the bulb, which was eventually dissipated to the environment from the outer surface of the lampshade.

For the bulb of design 2 with only a chimney, all of waste heat from the chips was imposed to the chimney, and then transferred from the chimney to the inner surface of the lampshade *via* natural convection (44%) and radiation (56%) heat transfer inside the bulb, which was finally dissipated to the environment from outer surface of the lampshade.

For the novel design 3 combining a metal block and a chimney, around 62% of the total waste heat was dissipated *via* the heat transfer path of *chips – metal base – metal block – environment*. While the remaining (38%) was taken away by the chimney, and then from the chimney to the lampshade *via* natural convection (18%) and radiation (20%) heat transfer inside the bulb, which was finally rejected to the environment from the lampshade surface.

In summary, there are two parallel heat transfer paths in a bulb: 1) direct heat conduction, *i.e., chips – metal base – metal block – environment, termed path 1 hereafter*; 2) indirect natural convection and radiation, *i.e., chips – metal base or chimney – lampshade – environment, termed path 2 hereafter*. The two paths co-exist in design 1 and 3 whilst only path 2 in design 2. Overall, the direct heat conduction (path 1) is more efficient than the indirect natural convection and radiation (path 2). For example, in design 1, the path 1 and path 2 stand for 81% and 19% of the total heat dissipation respectively, which are 62% and 38% respectively in design 3. For the indirect natural convection and radiation heat transfer inside the bulbs (path 2), the contribution of natural convection is slightly lower than radiation. It is worthy to note that, in design 2 and 3, the contribution of heat dissipation by path 2 is higher than that in design 1, due to the chimney enhances the natural convection and radiation heat transfer inside the bulbs.

4.1.3. Cooling capacity of the three designs of bulb

Since the reliability, lifespan and efficiency of LED chips all depend on the operating temperature, the maximum chip temperature is therefore used as the measure index to compare the cooling capacity of the three designs. Fig. 5 displays the maximum chip temperatures plotted as a function of heat dissipation for the three designs of bulbs filled with (a) air and (b) optimum gas mixture. At given heat dissipation, the design 3 yielded the lowest chip temperature, followed by the design 1 and design 2 sequentially. In other words, if the allowable temperature rise of chips is fixed, the design 3 can dissipate more heat.

4.2. Optimization of the conceptual design 3

As found in previous section, during the initial design the novel bulb configuration of design 3 outperformed the other two competitors. In this section, we shall show how to further enhance the cooling capacity of design 3 *via* distributing the chips properly and optimizing the geometry of the chimney.

4.2.1. Optimization of chip distribution

As shown in Fig. 4, the design 3 enables two heat dissipation paths: *chips – metal base – metal block – environment* (path 1) and *chips – chimney – lampshade – environment* (path 2). For each path the cooling capacity is limited. Therefore, in order to maximize the cooling capacity of the entire bulb, one should properly distribute thermal loads applied to the two paths to meet the individual cooling capacity of the two paths. To this end, the total 48 LED chips were systematically varied to place on the metal base and the chimney. Table 2 lists the different cases of chip distributions along with the predicted chip temperatures. The left digit in the case number of Table 2 means that the case was based on configuration of design 3 as shown in Fig. 1, while the right digit means the variation of chip distribution. Herein the total thermal load was fixed at 7 W at an ambient temperature of 300 K and the optimum gas mixture was filled in the bulb.

As shown in table 2, when the number of chips on the chimney was decreased from 40 to 8 (chips on the metal base increasing from 8 to 40 accordingly), both the maximum and average chip temperatures first decreased then increased. The maximum chip temperature achieved the lowest value of 354 K when 16 chips on the chimney and 32 chips on the metal base. This optimal chip distribution (16 on chimney and 32 on metal base) again shows that cooling capacity of the heat dissipation path 1 is larger than the path 2.

4.2.2. Optimization of chimney structure

In order to examine the effect of geometry of chimney on the cooling capacity, we compared four architectures of the chimney: 1) straight

Table 2
Simulation cases of different chip distributions on the chimney and metal base for the configuration of design 3.

Case	Number of LED chips		LED chip temperatures (K)	
	Chimney	Metal base	Maximum	Average
3–1	40	8	369.8	361.7
3–2	32	16	364.0	354.2
3–3	24	24	358.1	351.4
3–4	20	28	355.3	351.8
3–5	16	32	354.0	352.8
3–6	12	36	357.6	354.7
3–7	8	40	360.6	357.2

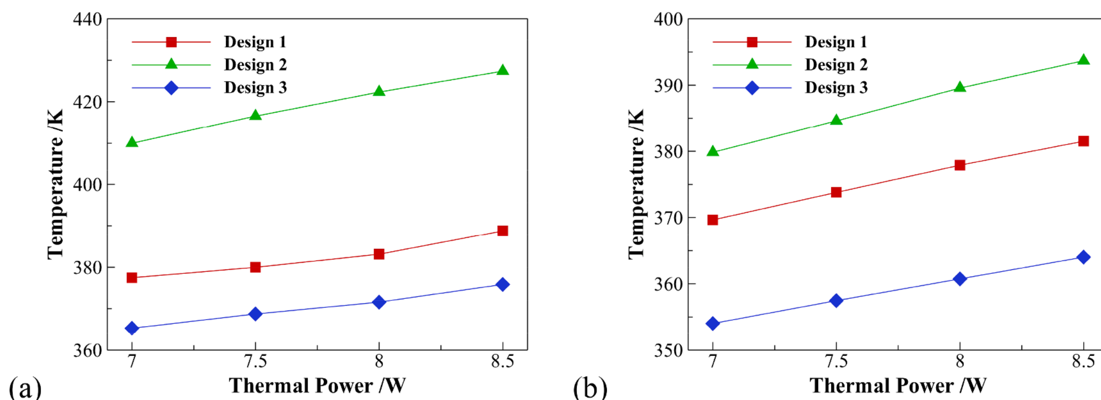

Fig. 5. Maximum chip temperatures plotted as a function of heat dissipation rate for the three bulbs filled with (a) air and (b) the optimum gas mixture.

chimney without bottom feet, *i.e.,* design 3; 2) straight chimney with four feet at the bottom, *i.e.,* design 3A; 3) chimney with contraction neck at the top but no bottom feet, *i.e.,* design 3B; 4) chimney with contraction neck at the top and bottom feet, *i.e.,* design 3C, as shown in Fig. 6(a). The top contraction neck was originally designed for locating chips on it to ensure uniform light emission from the bulbs. For the chimney design without top neck such as in design 3 and design 3A, light emission from the top of bulbs can be compensated by placing several chips at the center of the metal base. The chimney with four bottom feet such as in design 3A and design 3C can simplify the installation of the chimney and promote heat conduction between the chimney and the metal base.

Fig. 6(b) shows temperature distributions and flow streamlines in the bulbs of design 3, 3A, 3B and 3C. As shown in design 3B and 3C, the neck at top of the chimney hindered the flow circulation through the chimney which increased the temperature of chips located on the neck. Therefore, the top neck design is not ideal for the chimney structure. When comparing design 3 with design 3A, the bottom feet of chimney in design 3A enabled heat conduction between the chimney and metal base which can avoid local hot spot on the chimney and metal base.

Fig. 6(c) compares the maximum and average chip temperatures for the four chimney architectures. It is noted that the optimal chip distributions were found the same for the four architectures, *i.e.*, 16 chips on chimney and 32 chips on metal base. So results in Fig. 6(c) were all based on the optimal chip distribution. Clearly, the design 3A having straight chimney with bottom feet is optimal which can minimize the lowest chip temperature among the four chimney structures.

4.3. Comparison of the final design 3A with other bulbs

It has been found that the design 3A is the optimal design among the investigated architectures. What is the maximal cooling capacity of the best design? How about the cooling capacity of the optimal design when compared with the conventional bulb and commercial bulbs? In order to address these questions, the cooling capacity should be defined, *i.e.*, the maximal thermal power input of a bulb before the temperature of any chip reaching to the allowable operational temperature of 100–110 ℃ [10]. Take the allowable maximum chip temperature as 110 ℃ and the ambient temperature as 30 ℃, the allowable maximum chip temperature rise is then 80 ℃. Fig. 7(a) plots the rate of heat dissipation as a function of temperature rise for the bulbs of the final design 3A and the conventional bulb of design 1. As shown in the figure, given the allowable maximum chip temperature rise at 80 ℃, the cooling capacity of the final design 3A was 11.7 W against 7.4 W for the conventional design 1.

Commercial LED bulbs usually provide the maximal electrical power input rather than the maximum heat dissipation, *i.e.*, the cooling capacity. Before comparison with the commercial products can be made, one has to convert the maximal heat dissipation into the maximal

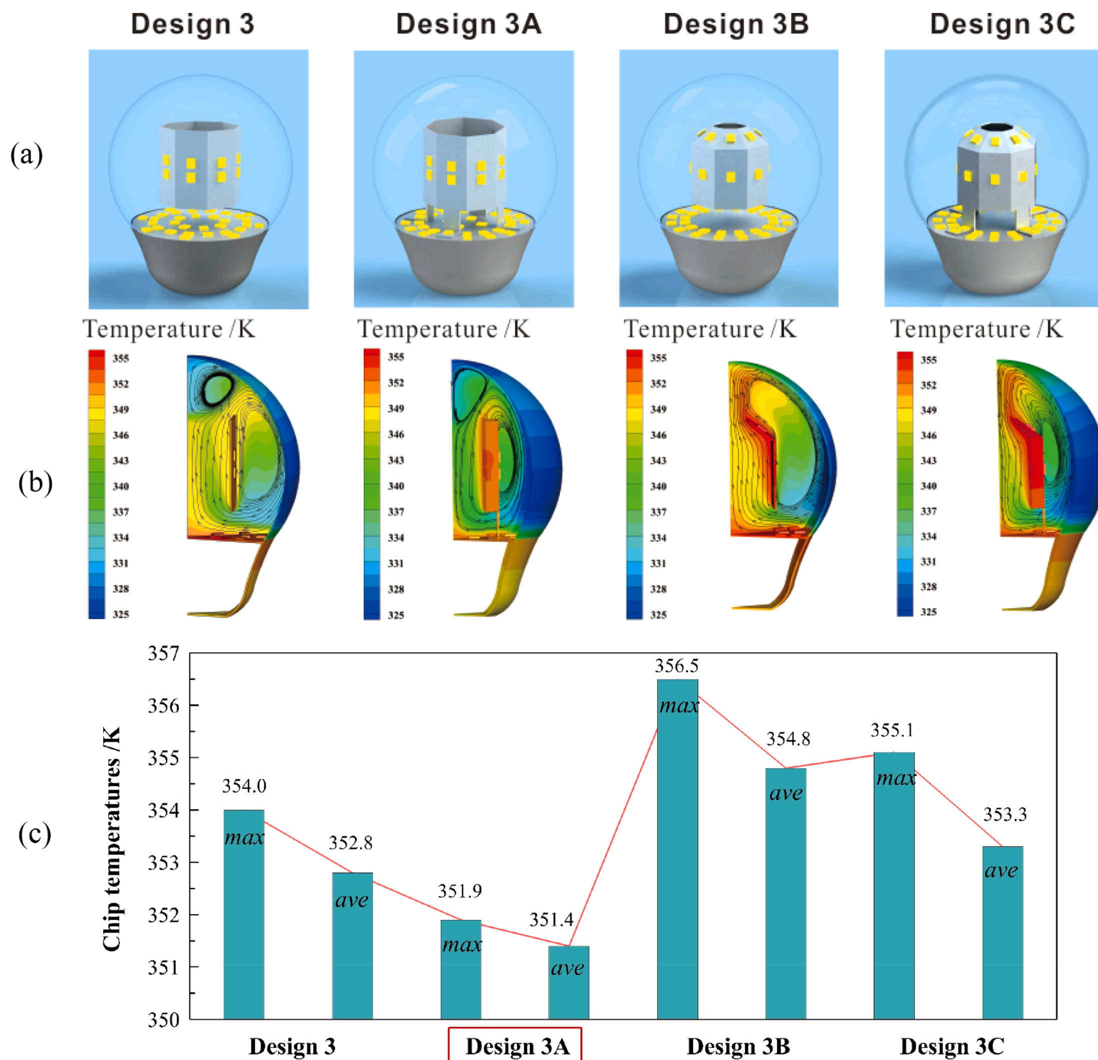

Fig. 6. Comparison of chimney architectures: (a) CAD drawing for the designs 3, 3A, 3B and 3C; (b) temperature and flow streamlines; (c) maximum and average chip temperatures; Results were obtained under conditions of: thermal load 7 W, ambient temperature 300 K and bulb filled with the optimum gas mixture.

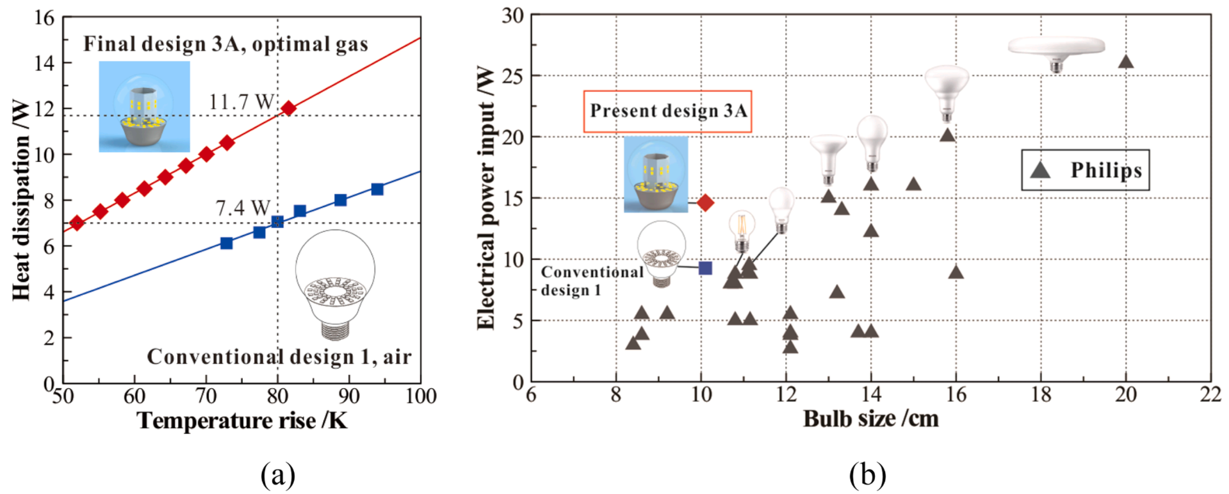

Fig. 7. Cooling capacity of the present final design 3A and the conventional design 1 (a) and comparison of the present bulbs with Philips bulbs (b).

electrical power input for the bulbs investigated in the study. Due to LEDs are not 100% efficient, much of the power running through an LED is output as heat and the rest is converted to light,

$$P_E = P_t / X_t \tag{9}$$

where P_E and P_t are the electrical power input and heat dissipation, respectively; X_t is the rate of input power to heat dissipation, which is usually between 75% and 80% whilst for some advanced LEDs it reduces to 50% to 60% [35]. To be conservative, assume LEDs convert 20% of the input power to light and 80% as heat. Accordingly, the maximal allowable power input of the final design 3A was calculated to be 14.6 W against 9.3 W for the conventional design 1.

Fig. 7(b) presents the electrical power input as a function of bulb size for the present final design 3A and conventional design 1 along with the Philips bulbs for comparison. If the efficiency of LEDs is fixed, the higher power input means more luminous flux output which is desirable. However, the bulb size and shape restriction forces a small heat sink which limits the cooling capacity and the power input of a bulb. Therefore, the strong drive in the design of bulb architecture is to increase the power input (or cooling capacity) as possible at given bulb size. Here we selected the maximum dimension such as height of bulb as the characteristic size for the comparison in Fig. 7(b).

As shown in Fig. 7(b) in general, the maximum power input of Philips bulbs increases with the bulb size due to surface area of heat sink increases. Remarkably, the maximum power input of the present final design 3A is 14.6 W in comparison to the maximum power input of 9.5 W for the Philips bulbs of similar size. Although it is difficult to know the exact definition of power input of Philips bulbs, *e.g.*, allowable chip temperature, ambient temperature, chip efficiency, the comparison between the present bulbs and Philips bulbs is still valuable. For example, the maximal power input of the present design 1 (9.3 W) is very close to the Philips bulbs (9.5 W) of the similar size, both have the same cooling architecture.

The novel cooling architecture proposed in the study containing an internal chimney and an external heat sink is an advantaged design compared to the conventional bulb with only an external heat sink. It is pointed out that, the study emphasizes the importance and how to activate the lampshade for heat dissipation rather than the reported value of cooling capacity of the novel bulb. Actually, the cooling capacity of the novel design can be further improved such as if adding some fins on the heat sink. Moreover, in addition to the LED bulbs the novel design strategy may be extended to other passive cooling scenarios such as indoor small cells for 5G communication.

5. Conclusions

A novel cooling architecture was proposed for LED chips which allows for the entire outer surface of the bulb dissipating heat to the environment efficiently. The novel design contains a chimney inside the bulb and a conventional heat sink where all chips are distributed onto the two components, enabling two parallel heat dissipating paths: *chips - heat sink - environment* (path 1) and *chips – chimney – lampshade – environment* (path 2). The two paths account for 62% and 38% of the total heat dissipation respectively, where the contribution from the path 2 is an additional gain of the novel bulb compared to the conventional design.

The cooling capacity of the novel bulb was optimized by properly distributing the number of chips to the metal base and the chimney. With the total number of chips fixed at 48, it was found that the distribution pattern of 16 chips on the chimney and 32 chips on the metal base results in the lowest chip temperature. Four architectures of the chimney were examined to investigate the effect of chimney geometry on the cooling capacity of the novel bulb, where the straight chimney with four bottom feet was found to be the optimal.

The novel bulb design has been compared with conventional design and Philips bulbs to demonstrate the advantage. It was found that at given heat dissipation the novel design could reduce the maximum chip temperature by 10–40 K compared to the conventional design while maintaining the size and shape. After optimization, the passive cooling capacity of the final design of the novel bulb is 1.57 times larger than the Philips bulbs of similar size and shape, thus allowing for more power input and more light output at given bulb size. Compared with conventional design, the novel LED bulb proposed in the study adds only a simple chimney structure inside the bulb; since the manufacture is easy and the material consumption is small, the cost of the new design is competitive. Most importantly, the novel design strategy may be extended to other passive cooling scenarios such as indoor small cells for 5G communication.

Declaration of Competing Interest

The authors declare that they have no known competing financial interests or personal relationships that could have appeared to influence the work reported in this paper.

Acknowledgements

This work was supported by the National Natural Science Foundation of China (51676156, 51206128, 51706178), the Postdoctoral Science

Foundation of China (2016M590942), the Shaanxi Province Science Foundation.

References

[1] L. Pérez-Lombard, J. Ortiz, C. Pout, A review on buildings energy consumption information, Energy Build. 40 (3) (2008) 394–398.
[2] N. Zografakis, K. Karyotakis, K.P. Tsagarakis, Implementation conditions for energy saving technologies and practices in office buildings: Part 1. Lighting, Renew. Sustain. Energy Rev. 16 (6) (2012) 4165–4174.
[3] N. Khan, N. Abas, Comparative study of energy saving light sources, Renew. Sustain. Energy Rev. 15 (1) (2011) 296–309.
[4] B.-L. Ahn, C.-Y. Jang, S.-B. Leigh, S. Yoo, H. Jeong, Effect of LED lighting on the cooling and heating loads in office buildings, Appl. Energy 113 (2014) 1484–1489.
[5] Alfonso Gago Calderón, Luis Narvarte Fernández, Luis Miguel Carrasco Moreno, Javier Serón Barba, LED bulbs technical specification and testing procedure for solar home systems, Renew. Sustain. Energy Rev., 2015, 41: 506-520.
[6] D. Jenkins, M. Newborough, An approach for estimating the carbon emissions associated with office lighting with a daylight contribution, Appl. Energy 84 (6) (2007) 608–622.
[7] W. Wang, Search on the development of LED industry in China, Modern Ind. Econ. Informationization 163 (7) (2018) 11–12 (in Chinese).
[8] B.-L. Ahn, J.-W. Park, S. Yoo, J. Kim, S.-B. Leigh, C.-Y. Jang, Savings in cooling energy with a thermal management system for LED lighting in office buildings, Energies 8 (7) (2015) 6658–6671.
[9] T. Cheng, X. Luo, S. Huang, S. Liu, Thermal analysis and optimization of multiple LED packaging based on a general analytical solution, Int. J. Therm. Sci. 49 (1) (2010) 196–201.
[10] J. Petroski, Advanced natural convection cooling designs for light-emitting diode bulb systems, J. Electron. Packag. 136 (4) (2014), 041005.
[11] Bladimir Ramos-Alvarado, Bo Feng, G.P. Peterson, Comparison and optimization of single-phase liquid cooling devices for the heat dissipation of high-power LED arrays, Appl. Therm. Eng., 2013, 59(1–2): 648-659.
[12] Yan Lai, Nicolás Cordero, Frank Barthel, Frank Tebbe, Jörg Kuhn, Robert Apfelbeck, Dagmar Würtenberger, Liquid cooling of bright LEDs for automotive applications, Appl. Therm. Eng. 29 (5-6) (2009) 1239–1244.
[13] Sheng Liu, Jianghui Yang, Zhiyin Gan, Xiaobing Luo, Structural optimization of a microjet based cooling system for high power LEDs, Int. J. Therm. Sci. 47 (8) (2008) 1086–1095.
[14] C.J.M. Lasance, András Poppe, Thermal management for LED applications, New York, Springer, 2014.
[15] Shou-Shing Hsieh, Yu-Fan Hsu, Meng-Lin Wang, A microspray-based cooling system for high powered LEDs, Energy Convers. Manage. 78 (2014) 338–346.
[16] Yueguang Deng, Jing Liu, A liquid metal cooling system for the thermal management of high power LEDs, Int. Commun. Heat Mass Transfer 37 (7) (2010) 788–791.
[17] S.F. Sufian, Z.M. Fairuz, M. Zubair, M.Z. Abdullah, J.J. Mohamed, Thermal analysis of dual piezoelectric fans for cooling multi-LED packages, Microelectron. Reliab. 54 (8) (2014) 1534–1543.
[18] Huaiyu Ye, Robert Sokolovskij, Henk W. van Zeijl, Alexander W.J. Gielen, Guoqi Zhang, A polymer based miniature loop heat pipe with silicon substrate and temperature sensors for high brightness light-emitting diodes, Microelectron. Reliab. 54 (6-7) (2014) 1355–1362.
[19] De-Shau Huang, Tzu-Ching Chen, Liang-Te Tsai, Ming-Tzer Lin, Design of fins with a grooved heat pipe for dissipation of heat from high-powered automotive LED headlights, Energy Convers. Manage. 180 (2019) 550–558.
[20] Daeseok Jang, Se-Jin Yook, Kwan-Soo Lee, Optimum design of a radial heat sink with a fin-height profile for high-power LED lighting applications, Appl. Energy 116 (2014) 260–268.
[21] Bin Li, Young-Jin Baik, Chan Byon, Enhanced natural convection heat transfer of a chimney-based radial heat sink, Energy Convers. Manage. 108 (2016) 422–428.
[22] Seung-Jae Park, Daeseok Jang, Se-Jin Yook, Kwan-Soo Lee, Optimization of a chimney design for cooling efficiency of a radial heat sink in a LED downlight, Energy Convers. Manage. 114 (2016) 180–187.
[23] Shangsheng Feng, Meng Shi, Hongbin Yan, Shanyouming Sun, Feichen Li, Tian Jian Lu. Natural convection in a cross-fin heat sink, Appl. Therm. Eng., 2018, 132: 30-37.
[24] Shangsheng Feng, Feichen Li, Fenghui Zhang, Tian Jian Lu, Natural convection in metal foam heat sinks with open slots, Exp. Therm. Fluid Sci., 2018, 91: 354-362.
[25] A. Bhattacharya, R.L. Mahajan, Metal foam and finned metal foam heat sinks for electronics cooling in buoyancy-induced convection, J. Electron. Packag. 128 (3) (2006) 259–266.
[26] Shangsheng Feng, Jiujie Kuang, Ting Wen, Tian Jian Lu, Koichi Ichimiya, An experimental and numerical study of finned metal foam heat sinks under impinging air jet cooling, Int. J. Heat Mass Transfer, 2014, 77: 1063-1074.
[27] Seong Rim Nam, Chung Woo Jung, Chang-Hwan Choi, Yong Tae Kang, Cooling performance enhancement of LED (light emitting diode) packages with carbon nanogrease, Energy, 2013, 60: 195-203.
[28] H.J. Han, Y.I. Jeon, S.H. Lim, W.W. Kim, K. Chen, New developments in illumination, heating and cooling technologies for energy-efficient buildings, Energy 35 (6) (2010) 2647–2653.
[29] Daeseok Jang, Seung-Jae Park, Kwan-Soo Lee, Thermal performance of a PCB channel heat sink for LED light bulbs, Int. J. Heat Mass Transf. 89 (2015) 1290–1296.
[30] Shangsheng Feng, Shanyouming Sun, Hongbin Yan, Meng Shi, Tian Jian Lu, Optimum composition of gas mixture in a novel chimney-based LED bulb, Int. J. Heat Mass Transfer, 2017, 115: 32-42.
[31] https://www.usa.lighting.philips.com/consumer/p/led-bulb.
[32] Shangsheng Feng, Feng Xu, A LED bulb with optimum heat dissipation structure and chips distribution, Chinese Patent, 201920608378.8.
[33] ANSYS FLUENT 14.5 user's & tutorial guide, ANSYS Inc., Canonsburg, PA, 2012.
[34] Theodore L. Bergman, Frank P. Incropera, Adrienne S. Lavine, David P. DeWitt, Introduction to heat transfer, sixth ed., John Wiley & Sons, Jefferson City, 2011.
[35] https://www.cree.com/led-omponents/media/documents/XLampThermalManagement.pdf.